1706

Simultaneous Measurement of Pore and Elastic Properties of Rocks Under Triaxial Stress Conditions

BERNHARD WILHELMI
DEMAG-LAUCHHAMMER
DUSSELDORF-BENRATH, GERMANY

WILBUR H. SOMERTON
MEMBER AIME
U. OF CALIFORNIA
BERKELEY, CALIF.

ABSTRACT

Simultaneous measurement of pore and elastic properties of rocks under a wide range of triaxial stress conditions may be made with equipment and methods developed in this paper. Tests were run on three outcrop sandstones at several confining pressures and axial stresses up to approximately 80 percent of failure stress. The greater reduction in porosities and permeabilities occurred in the hydrostatic loading portion of the stress cycle, but substantial reductions in both properties did occur upon application of deviator (triaxial) stress.

Triaxial elastic moduli were calculated from strain gauge measurements. Both Young's moduli and shear moduli were found to increase with increasing confining pressure. Poisson's ratios increased with axial stress but showed no consistent change with confining pressure. Only very general relations were observed between pore and elastic properties. The lesser decrease in porosity and permeability at higher stress values is related to increase in rigidity of rocks at higher stresses.

INTRODUCTION

Many investigators have studied the effects of hydrostatic stress on the properties and behavior of rocks. A few have studied the effects of triaxial stress fields on individual physical properties of rocks. To our knowledge no one has measured simultaneously pore and elastic properties of rocks under a wide range of triaxial stress conditions. This is the purpose of this work.

Rocks exist in the subsurface under what Jaeger[1] refers to as "polyaxial" stress conditions (all principal stresses unequal). When two of the three principal stresses are equal, this is referred to as triaxial loading. The triaxial method of loading is most commonly used in modern testing work because experimental difficulties in measuring physical properties of rocks are greatly reduced over polyaxial testing. Although triaxial loading may not reproduce subsurface conditions precisely, subsurface stress conditions are never known precisely anyway. Triaxial testing would seem to be more realistic than testing under hydrostatic loading (all principal stresses equal) for application of results to subsurface problems.

The objectives of this work were threefold: (1) to develop methods of measuring simultaneously pore and elastic properties of rocks under triaxial stress conditions, (2) to determine whether changes in these properties are of sufficient magnitude to be considered in subsurface calculations and (3) to attempt to relate changes in pore properties and elastic properties since they will have been measured at the same time under identical loading conditions.

REVIEW OF EARLIER WORK

PORE PROPERTIES

Several investigators have studied the effects of stress on the physical properties of rocks. Fatt and Davis[2] showed the reduction of permeability of rock with hydrostatic loading. McLatchie *et al.*[3] and Knutson and Bohor[4] related permeability reduction to compressibility of reservoir rock, again under hydrostatic loading. Wyble,[5] and later Redmond,[6] evaluated the effects of applied radial pressure on conductivity, porosity and permeability of sandstones. In this latter work, no axial stress was applied.

Dobrynin[7] reviewed much of the previous work done on the effects of overburden pressure on physical properties of rocks. He concluded that changes in physical properties are controlled to a large extent by pore compressibility of the rock. Several sets of curves developed from empirical relations are presented. These curves permit estimation of change of properties with net overburden pressure, knowing the pore compressibility and porosity of the rock. Net overburden pressure is defined as $(P_e - 0.85P_i)$ where P_e is the

Original manuscript received in Society of Petroleum Engineers office Dec. 6, 1966. Revised manuscript received June 16, 1967. Paper (SPE 1706) was presented at SPE Third Conference on Rock Mechanics held in Austin, Tex., Jan. 25-26, 1967.

[1]References given at end of paper.

hydrostatic pressure to which the samples were subjected and P_i is the pore pressure.

Bergamini[8] studied the effects of nonuniform stress on permeability of sandstones. Radial confining pressure and axial stress were applied independently of each other. Tests were run on a number of sandstones where first the radial and axial stresses were increased equally (hydrostatic loading) and then the axial stress was maintained constant while the radial pressure was increased. Permeabilities were measured at 500-psi increments to a maximum value of 4,000 psi. Reduction of permeability of the order of 10 percent was observed for most sandstones tested. One low-permeability sandstone containing considerable clay showed permeability reductions of nearly 50 percent.

In further analysis of Bergamini's data, Gray *et al.*[9] compared permeability reduction at hydrostatic stress with the reduction when axial stress was only one-third of the applied radial stress. There was less change in permeability under the nonuniform stress condition than under uniform (hydrostatic) stress. If the nonuniform stress is expressed in terms of a mean effective stress $(\sigma_y + 2\sigma_x)/3$, where σ_y is the axial stress and σ_x the the radial stress, the apparent difference in permeability still exists but is reduced in magnitude.

Handin and co-workers measured the changes in porosity of various rocks under triaxial loading conditions.[10] However, only final results at the completion of the tests are given and thus a relation between triaxial stress and change in porosity was not obtained.

ELASTIC PROPERTIES

Cleary[11] presented the most nearly complete data on the elastic properties of sandstones. Tests were run under triaxial loading conditions to determine Young's modulus and Poisson's ratio, and from these other elastic parameters were calculated. In determining Young's modulus and Poisson's ratio, Cleary assumed that Hooke's law applied for the special conditions of the tests. The conditions of the tests were as follows: initial values of radial and axial stress were first applied and strain readings recorded; the axial stress was then increased to a new value keeping the radial stress constant, and new values of strain were recorded; the axial stress was returned to its original value and a check was made to assure that the strains returned to very nearly their original values. Young's modulus was calculated as the change in axial stress divided by change in axial strain and Poisson's ratio as the ratio of the change in lateral strain to the change in axial strain. The mean effective stress at which these values of E and υ are assumed to apply is given by $\bar{\sigma} = \left[\frac{2\sigma_x + (\sigma_{y1} + \sigma_{y2})/2}{3}\right]$, where σ_x = radial stress, σ_{y1} = axial stress, original, and σ_{y2} = axial stress, new.

The disadvantage of the above technique for obtaining elastic data from triaxial tests is that the results are not clearly related to specific triaxial states of stress. In fact, the results are more closely related to an equivalent hydrostatic state of stress.

Uniaxial elastic moduli can be related to triaxial states of stress by the following equations which are readily derived from Hooke's law.[12]

$$E = \frac{(\sigma_y - \sigma_x)I_1}{\epsilon_y I_1 - \sigma_x J_1} \quad \ldots\ldots\ldots\ldots (1)$$

$$\upsilon = \frac{\sigma_y \epsilon_x - \sigma_x \epsilon_y}{\epsilon_y I_1 - \sigma_x J_1} \quad \ldots\ldots\ldots\ldots (2)$$

where σ_y = axial stress
$\sigma_x = \sigma_z$ = lateral stress
ϵ_y = axial strain
$\epsilon_x = \epsilon_z$ = lateral strain
$I_1 = \sigma_y + \sigma_x + \sigma_z = \sigma_y + 2\sigma_x$
$J_1 = \epsilon_y + \epsilon_x + \epsilon_z = \epsilon_y + 2\epsilon_x$.

Also, if shear modulus G is defined in the usual manner,

$$G = \frac{E}{2(1+\upsilon)} \quad \ldots\ldots\ldots\ldots (3)$$

it can be shown that[12]

$$G = \tfrac{1}{2}\frac{(\sigma_y - \sigma_x)}{(\epsilon_y - \epsilon_x)} \quad \ldots\ldots\ldots\ldots (4)$$

Triaxial test data are generally expressed in simpler form than the above equations.[13] Deviator stresses are employed but strains are generally referenced to zero at hydrostatic loading equivalent to the applied confining pressure. Thus, the triaxial Young's modulus, Poisson's ratio and shear modulus are

$$E_{TR} = \frac{(\sigma_y - \sigma_x)}{\epsilon_{yTR}} \quad \ldots\ldots\ldots (5)$$

$$\upsilon_{TR} = \frac{\epsilon_{xTR}}{\epsilon_{yTR}} \quad \ldots\ldots\ldots\ldots (6)$$

$$G_{TR} = \tfrac{1}{2}\frac{(\sigma_y - \sigma_x)}{(\epsilon_{yTR} - \epsilon_{xTR})} \quad \ldots\ldots\ldots (7)$$

where $(\sigma_y - \sigma_x)$ = deviator stress
ϵ_{yTR} = triaxial longitudinal strain
ϵ_{xTR} = triaxial lateral strain.

EQUIPMENT AND MEASURING METHODS

Conventional triaxial loading equipment used to simulate subsurface stress conditions was provided with special attachments to allow measurement of pore properties at the same time elastic properties were being measured. The apparatus is best described by dividing it into five groupings: (1) high-pressure cell, (2) loading machine, (3) confining pressure system, (4) strain measuring devices and (5) porosity and permeability measuring apparatus.

HIGH-PRESSURE CELL

The triaxial cell was similar to that designed by the U. S. Bureau of Reclamation. Parts of the cell are shown in Fig. 1 and the assembled cell is shown in place in the testing machine in Fig. 2. The loading head is provided with strain gauge terminals and outlets for the steel tubing used to measure pore properties. Neoprene rubber tubing 1/16 in. thick was used to transmit the confining pressure to the core. This tubing proved to be entirely satisfactory as long as care was taken to prevent damage to the strain gauges and lead wires when the tubing was mounted onto the core. After mounting the core, a leak test was made by applying vacuum to the core through the tubing provided for pore properties measurements. If a vacuum of 100 microns could be maintained, the seal was considered to be satisfactory.

A minor objection to this triaxial cell is the large area of the head over which the confining pressure acts to give a magnified value of axial load. It was necessary to apply a correction to the apparent axial load by the amount $(A_b \times P_x)$ where A_b is the annular area of the loading head to which confining pressure P_x is applied.

LOADING MACHINE

The loading machine used was a 160,000-lb screw-power testing machine. There are five scale ranges with a stated accuracy of ± 0.125 percent of full scale for each of the ranges. No particular difficulties were encountered with this machine and it was a simple matter to control the axial stress and hold it constant over the period of the tests.

CONFINING PRESSURE SYSTEM

The hydraulic system used to control the confining pressure on the sample is shown schematically in Fig. 3. Principal control is obtained by means of an air-operated pump. It is possible to maintain a set pressure in the system to ± 10 psi. A motor-driven pump is included in the system to allow rapid filling of the cell and circulation of oil to remove air from the system. A sight tube is provided to give visual evidence of the elimination of air from the system.

Several pressure gauges are provided in the system to allow accurate pressure readings in any pressure range. A 6,000-psi pressure gauge with a least reading of 10 psi was later added to the system to improve further the reading and control of pressure.

STRAIN MEASURING DEVICES

Axial and lateral strains were measured by means of resistance wire strain gauges cemented

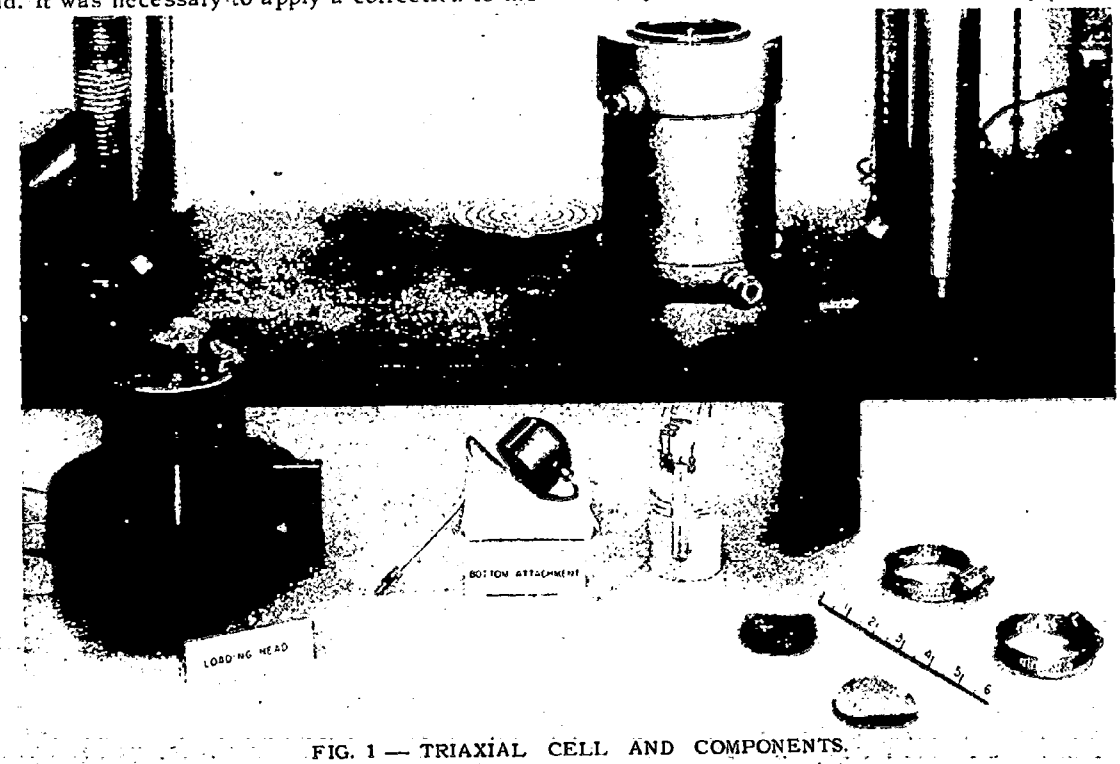

FIG. 1 — TRIAXIAL CELL AND COMPONENTS.

to the test specimens. Two strain gauges, which have effective lengths of 1¾ in. and negligible cross-sensitivity, were mounted diametrically opposite each other along the length of the sample. A second pair was mounted circumferentially in the middle of the sample to give lateral strains. The two pairs of gauges were connected in series and were connected to two strain indicators in a half-bridge circuit. Compensating gauges were mounted on a dummy core to provide for temperature compensation. The strain gauge indicators have a least count of 1 micro-in./in. so that very small strains could be read with good accuracy.

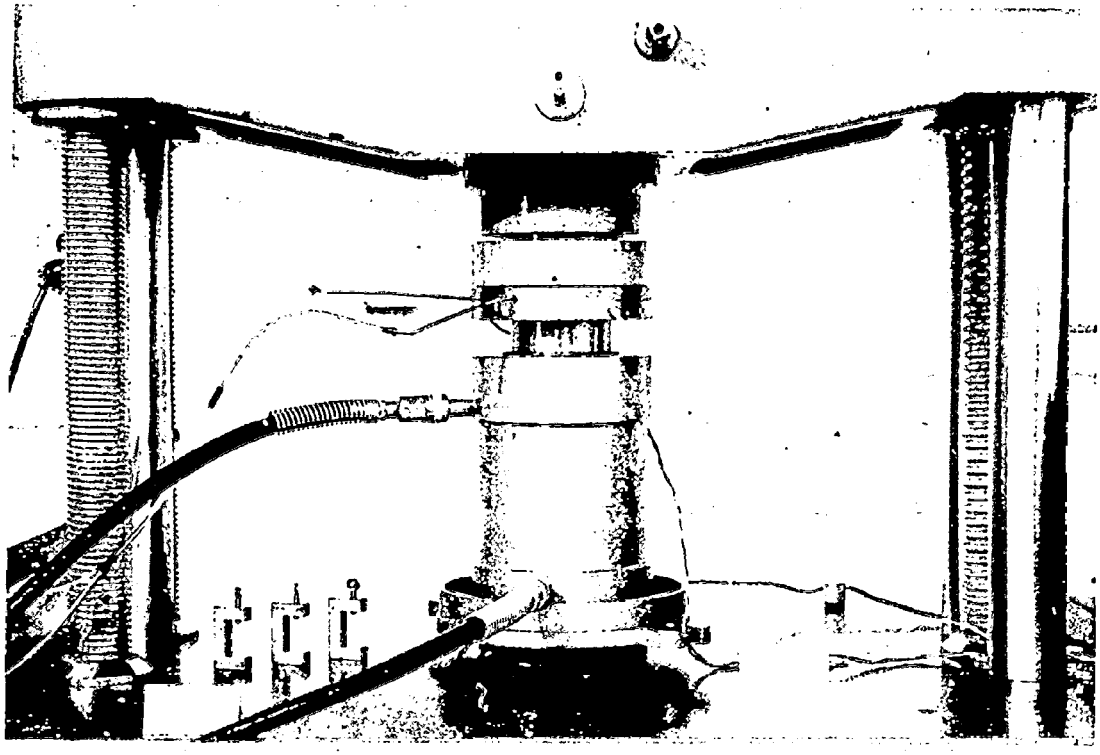

FIG. 2 — TRIAXIAL CELL ASSEMBLED.

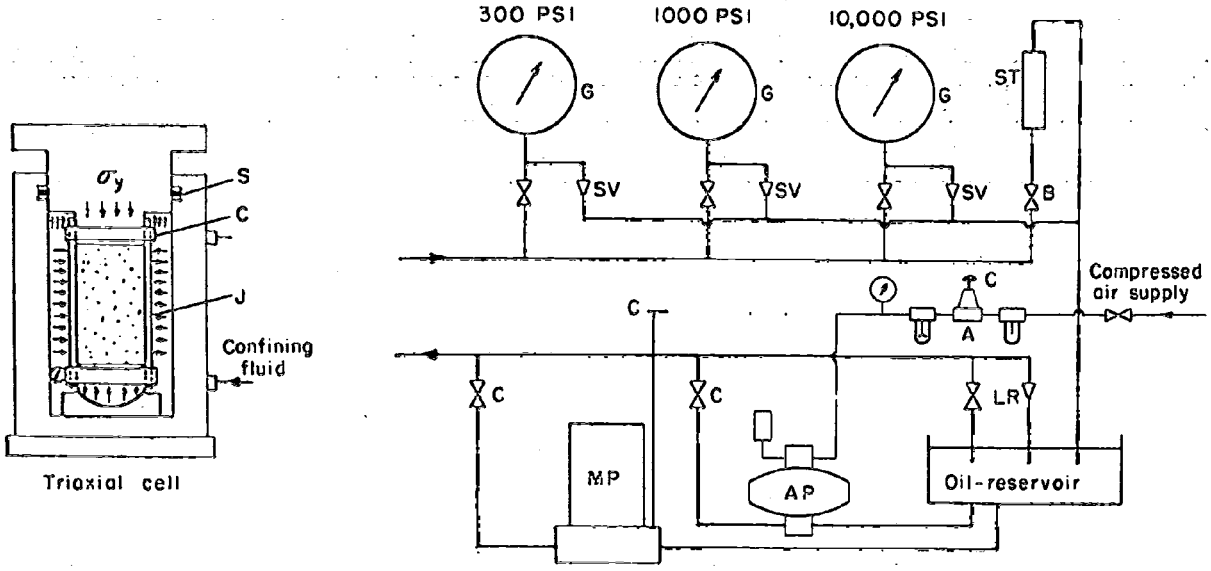

S Seal MP Motor driven pump LR Load release valve B Bleed valve
C Clamp AP Air driven pump SV Safety valves C Control valves
J Jacket G High press. gauges ST Sight tube A Air control unit

FIG. 3 — DIAGRAM OF CONFINING PRESSURE SYSTEM.

POROSITY AND PERMEABILITY MEASURING DEVICES

The pore property measuring equipment is based on a design developed by Yamasaki (Fig. 4).[14] To measure porosity of the sample, the pore volume is determined as follows. Valve V_3 and three-way cock C are closed, valves V_1 and V_2 are opened and the system is evacuated to 100 microns as indicated by the vacuum gauge. The mercury level in burette B is adjusted to zero with cock C open to the atmosphere. Valve V_2 is then closed and cock C is turned to admit air to the evacuated system. The mercury level in the burette is then raised to restore atmospheric pressure in the system as indicated by manometer M_1. The volume of air displaced is recorded. In a previous test, the amount of dead space in the evacuated system was determined by running the above test on a lucite cylinder of the same size as the test specimen but containing an axial hole of known volume to allow air passage through the system. The dead space volume, corrected for the volume of the axial hole was subtracted from the volume determined for the test specimen to give the pore volume. Porosity of the test sample was determined from the pore volume and the original bulk volume of the sample corrected for the known axial and lateral strains.

Permeability was determined by opening valves V_1 through V_3, closing cock C and drawing air through the core by running the vacuum pump. The volume rate of air flow was measured by means of the capillary flow meter. Pressure drop across the system was measured by manometers M_1 and M_2.

TABLE 1 — AVERAGE ORIGINAL PROPERTIES OF SANDSTONES

Property	Bandera	Berea	Boise
Porosity, percent	22	19	28
Permeability, md	14	160	1,700
Sonic velocity, ft/second	10,000	7,500	8,900
Compressive strength, psi	7,600	8,200	5,100
Young's modulus, psi*	1.9×10^6	2.3×10^6	2.8×10^6
Poisson's ratio*	0.16	0.185	0.32

*Measured in uniaxial test at 50 percent of compressive strength.

To obtain pressure drop across the core, it was necessary to evaluate losses in the lines between the manometers and the top and bottom of the core, respectively. These losses were determined as functions of flow rate in separate tests. Appropriate corrections were made to the manometer readings, pressure loss across the length of the core was determined and the mean pressure in the core was calculated. These data, along with physical properties of the flowing fluid, made possible the calculation of permeability.

SAMPLE PREPARATION

Three well-known and commercially available sandstones (Bandera, Berea and Boise) were used for these tests. Typical values of physical characteristics of the sandstones are given in Table 1. Although the sandstones are quite uniform in characteristics, care was taken to obtain adjacent cores from the same block.

Cores of the three sandstones were drilled perpendicular to the bedding planes with a 2-in. diamond core bit. The cores were trimmed to 4 in.

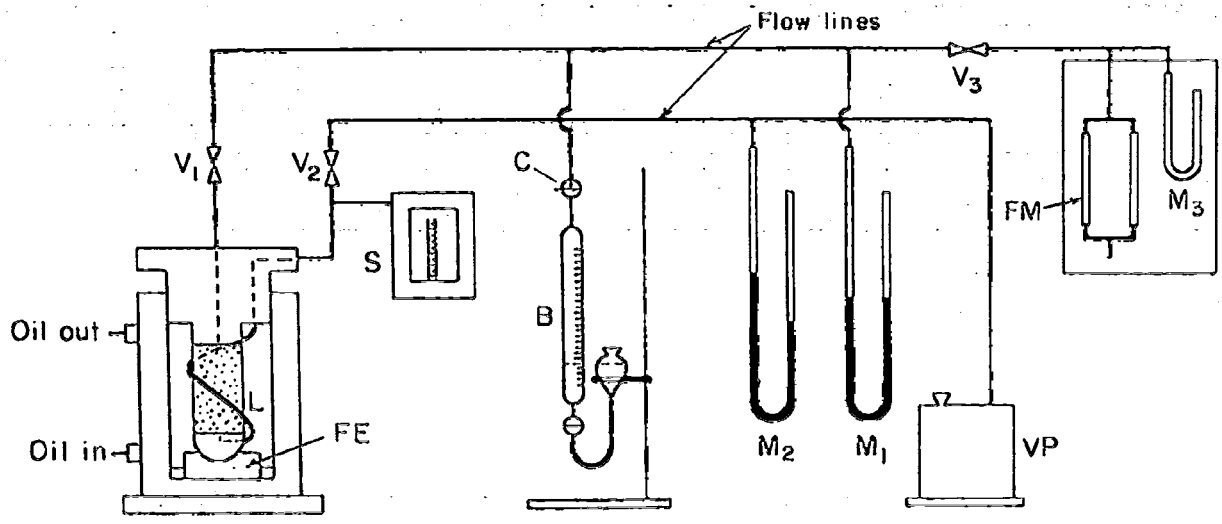

C_1 Three way cock	B Burette	S Stokes gauge
V_1 Control valve	L Flexible tubing	M_1, M_2 Manometers
V_2 Control valve	FE Force equalizer	M_3 Manometer, flow meter
V_3 Control valve	VP Vacuum pump	FM Capillary flow meter

FIG. 4 — POROSITY AND PERMEABILITY MEASURING DEVICE.

in length with a diamond saw. The ends of the cores were ground flat and parallel and did not deviate by more than ½° from perpendicular to the axis of the cylinder. The cores were dried in an oven at 210 ± 10F for 24 hours and were allowed to cool to room temperature in a vacuum oven.

Strain gauges were mounted on the cores as indicated earlier — two axial gauges and two circumferential. Mounting surfaces were prepared by first applying one or two thin coats of cement, depending upon the roughness of the surface. The cemented gauges were held in place by means of a clamping device and were dried in an oven at 190 ± 10F for 24 hours. Foil terminals were mounted on the samples for connecting strain gauges to lead wires. Lead wires to the loading head were of 26-gauge constantan wire to provide adequate strength and were insulated with enamel and lacquer-coated cotton. When all strain gauge leads were installed and tested, the neoprene sleeve was applied to the core and the leak test was conducted as previously indicated.

PRELIMINARY TESTS

A series of tests was run on samples of the three sandstones to determine ultimate compressive strengths under triaxial loading conditions. These results are given in Table 2 for the four confining pressures used in subsequent tests (500, 1,000, 2,000 and 4,000 psi).

Base values of porosity and permeability of each sample were determined before triaxial tests were run. These were measured with the core in the cell and with 100-psi hydrostatic pressure applied. This amount of pressure was necessary to seal the neoprene tubing about the core and to eliminate any dead volume around the core. All other values of porosity and permeability were referenced to these initial or base values.

MEASURING METHOD

Previous experience has shown [15] that strain stabilization of stress-relaxed outcrop samples can be achieved only by repeated loading and unloading. Fig. 5 shows the near stabilization of strain in a sample on the fifth loading cycle. Therefore, the standard procedure was to apply the desired confining pressure to the sample and then load axially to approximately 75 percent of the failure stress. After 15 minutes the axial load was released and the sample returned to hydrostatic loading. This was repeated for three additional cycles and measurements were then made on the fifth loading cycle. During initial loading cycles, strain gauge readings were taken only at the ends of the cycle to confirm that strain stabilization was being achieved.

At the start of the fifth loading cycle, pore volumes and flow rates were measured at the hydrostatic loading condition. To allow adequate time for strain stabilization, axial and lateral strain readings were recorded just prior to increasing the load. Axial stress was then increased in increments of 1,000 psi and pore volumes, flow rates and strains were measured at each stress level. Measurements were continued until a stress of approximately 80 percent of the ultimate strength was reached. The axial stress was then released and the sample returned to hydrostatic loading condition. Pore volumes, flow rates and strains were measured again to assure that the sample had not changed its character during the loading cycle.

TABLE 2 — TRIAXIAL COMPRESSIVE STRENGTHS

Confining Pressure (psi)	Bandera (psi)	Berea (psi)	Boise (psi)
500	9,500	16,000	6,800
1,000	11,300	20,000	9,200
2,000	14,900	25,300	10,100
4,000	20,900	33,600	14,200

EXPERIMENTAL RESULTS

PORE PROPERTIES

Results of pore properties measurements are plotted as functions of deviator stress in Figs. 6 through 11. Porosities and permeabilities are expressed as percentages of the base values. Base values were measured in the cell at 100-psi hydrostatic load. Deviator stress is the difference between the variable axial stress and the constant confining stress. Zero deviator stress represents the condition of hydrostatic loading at the particular confining pressure. The pore property values at zero deviator stress are hydrostatic loading values.

Reduction in porosity under triaxial loading conditions was small — of the order of 5 to 8 percent of the porosity value. In other words, the reduction was 1 to 2 porosity percent. The greater part of the porosity reduction occurred during the hydrostatic loading portion of the cycle. However, application of deviator stress caused further reduction in porosity in all cases and in some cases the reduction was equal in amount to that caused by hydrostatic loading.

Good reproducibility of porosity measurement results is indicated by repeat measurements on the

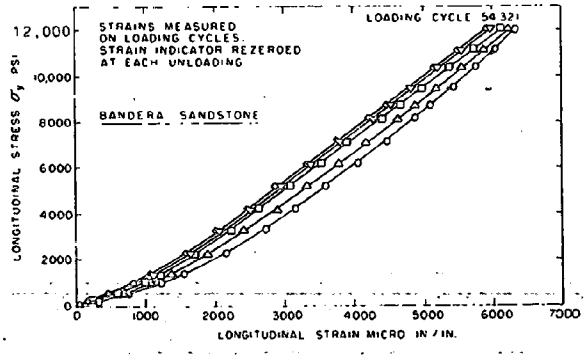

FIG. 5 — STRESS-STRAIN BEHAVIOR OF BANDERA SANDSTONE UNDER CYCLIC LOADING.

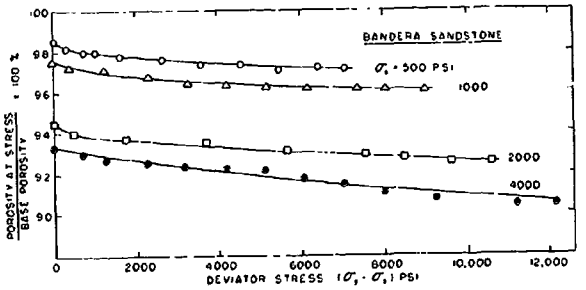

FIG. 6 — POROSITY AS A FUNCTION OF DEVIATOR STRESS WITH CONFINING PRESSURE AS A PARAMETER.

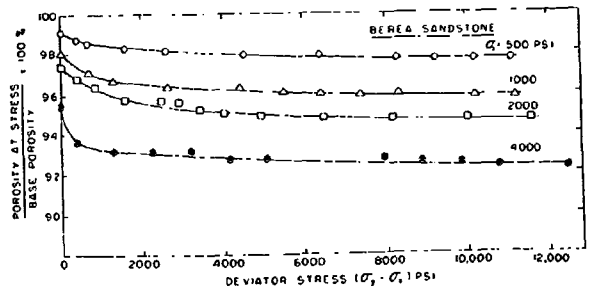

FIG. 7 — POROSITY AS A FUNCTION OF DEVIATOR STRESS WITH CONFINING PRESSURE AS A PARAMETER.

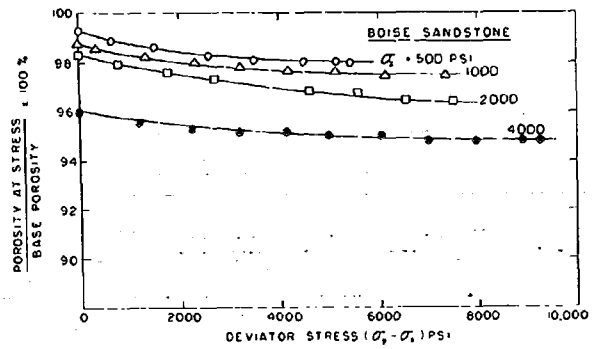

FIG. 8 — POROSITY AS A FUNCTION OF DEVIATOR STRESS WITH CONFINING PRESSURE AS A PARAMETER.

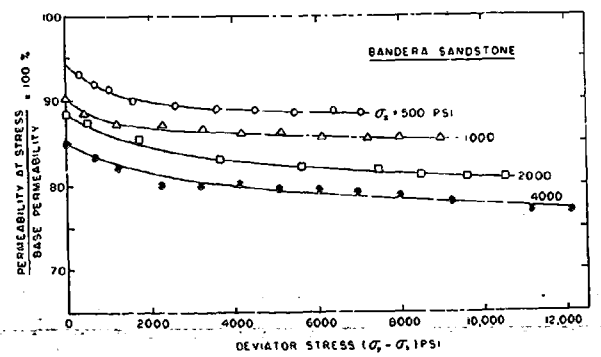

FIG. 9 — PERMEABILITY AS A FUNCTION OF DEVIATOR STRESS WITH CONFINING PRESSURE AS A PARAMETER.

fourth and fifth loading cycles as shown in Fig. 12. Changes in porosity for successive stress increments were so small as to approach the limit of capability of the measuring equipment. Consequently, smooth curves were drawn through the data points rather than giving credence to the apparent irregularities in the data.

Changes in permeability under triaxial loading were of much greater magnitude than changes in porosity. Reductions were of the order of 10 to 20 percent for Berea and Bandera sandstones and were as high as 65 percent for Boise sandstone.

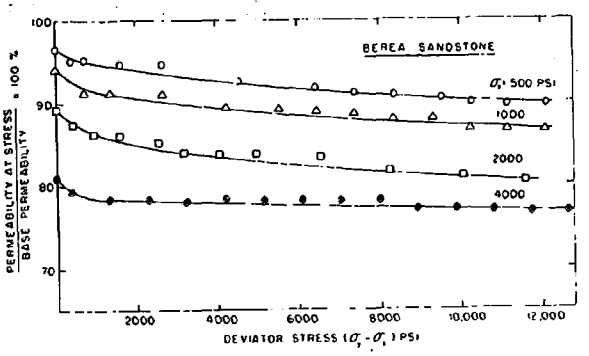

FIG. 10 — PERMEABILITY AS A FUNCTION OF DEVIATOR STRESS WITH CONFINING PRESSURE AS A PARAMETER.

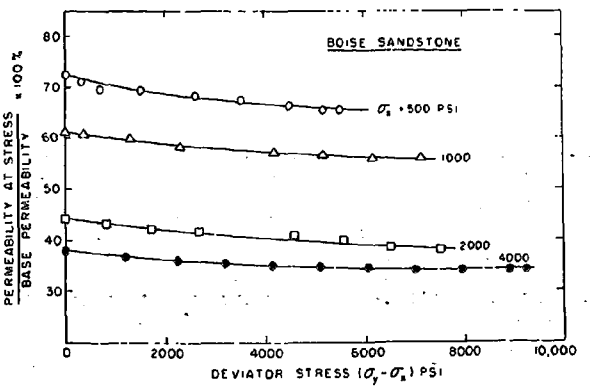

FIG. 11 — PERMEABILITY AS A FUNCTION OF DEVIATOR STRESS WITH CONFINING PRESSURE AS A PARAMETER.

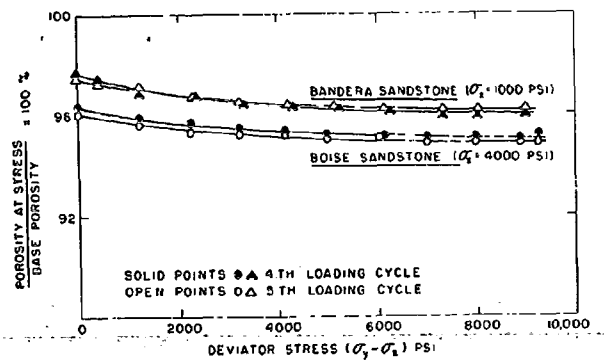

FIG. 12 — REPRODUCIBILITY OF POROSITY MEASUREMENTS ON BANDERA AND BOISE SANDSTONE FOR FOURTH AND FIFTH LOADING CYCLES.

Although again the greatest change occurred in the hydrostatic loading part of the cycle, substantial additional reduction in permeability occurred upon application of deviator stress. Reproducibility of permeability results was good as indicated by repeat measurements for the fourth and fifth loading cycles shown in Fig. 13. Smooth curves were drawn through the data points since changes in permeability for successive stress increments again approached the limit of capability of the measuring equipment.

ELASTIC MODULI

Deviator stress vs triaxial longitudinal strain data are plotted for the three sandstones in Figs. 14 through 16. At 4,000-psi confining pressure, these data plot as straight lines for all three sandstones. At lower values of confining pressures the lines show some curvature initially but tend to become linear at higher deviator stresses, approaching at the limit the slopes of the 4,000-psi confining pressure lines. Slopes of the straight portions of these lines are taken as the Young's moduli and are reported in Table 3. Values of Young's moduli calculated from Eq. 1 are also given in the table for comparison. These latter values are the average of values calculated for the straight-line portions of the data.

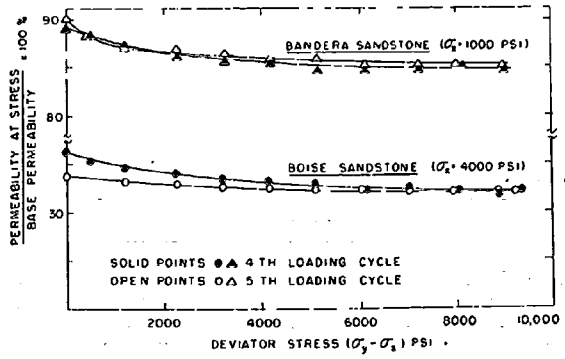

FIG. 13 — REPRODUCIBILITY OF PERMEABILITY MEASUREMENTS ON BANDERA AND BOISE SANDSTONE FOR FOURTH AND FIFTH LOADING CYCLES.

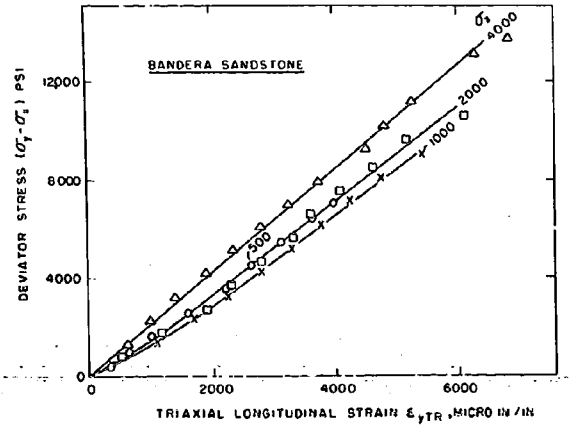

FIG. 14 — DETERMINATION OF YOUNG'S MODULUS, BANDERA SANDSTONE.

TABLE 3 — MEASURED AND CALCULATED ELASTIC MODULI

Sample	Lateral Stress σ_x (psi)	Young's Modulus E (psi)	Young's Modulus E_{TR}	Shear Modulus G (psi)	Shear Modulus G_{TR}	Poisson's Ratio ν	Poisson's Ratio ν_{TR}
Bandera	500	1.58×10^6	1.90×10^6	$.67\times10^6$	$.70\times10^6$	.19	.36
	1,000	1.47×10^6	1.86×10^6	$.62\times10^6$	$.71\times10^6$	.19	.29
	2,000	1.54×10^6	1.90×10^6	$.65\times10^6$	$.73\times10^6$	.18	.25
	4,000	1.72×10^6	2.10×10^6	$.73\times10^6$	$.85\times10^6$	.21	.22
Berea	500	2.5×10^6	3.5×10^6	$.90\times10^6$	$.90\times10^6$	.39	.97 ?
	1,000	2.7×10^6	3.7×10^6	1.13×10^6	1.29×10^6	.19	.47 ?
	2,000	2.7×10^6	3.9×10^6	1.24×10^6	1.50×10^6	.09 ?	.28
	4,000	3.3×10^6	4.1×10^6	1.44×10^6	1.69×10^6	.15	.26
Boise	500	1.80×10^6	1.80×10^6	$.74\times10^6$	$.75\times10^6$	.21	.24
	1,000	1.81×10^6	1.80×10^6	$.72\times10^6$	$.70\times10^6$	.25	.30
	2,000	2.10×10^6	1.85×10^6	$.85\times10^6$	$.77\times10^6$	.24	.20
	4,000	2.00×10^6	1.85×10^6	$.81\times10^6$	$.80\times10^6$	.24	.21

Figs. 17 through 19 show plots of deviator stress vs deviator strain data for the three sandstones. Values of $(\epsilon_y - \epsilon_x)$ rather than $(\epsilon_{yTR} - \epsilon_{xTR})$ were plotted to show the displacement of the plots from the origin. This displacement shows the difference in longitudinal and lateral strains at conditions of hydrostatic loading $(\sigma_y - \sigma_x = 0)$ and is a measure of strain anisotropy. It should be noted that both Bandera and Berea sandstones show strain anisotropy but Boise does not.

The plots of deviator stress vs deviator strain data are straight lines in nearly all cases, the slopes of which are two times the shear modulus G_{TR}. Values of G_{TR} are shown in Table 3 and

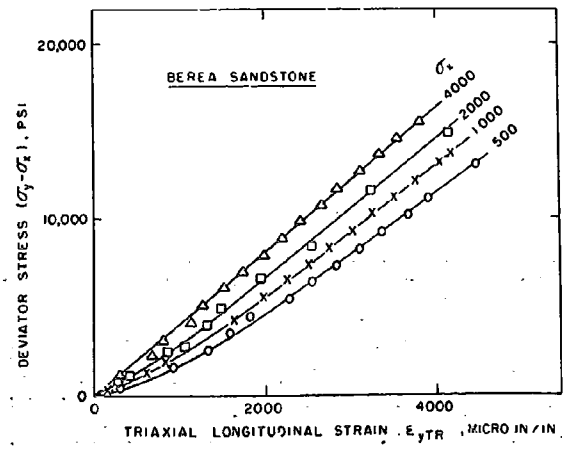

FIG. 15 — DETERMINATION OF YOUNG'S MODULUS, BEREA SANDSTONE.

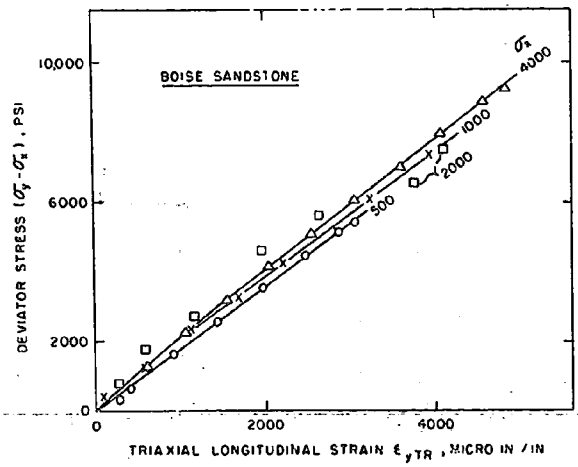

FIG. 16 — DETERMINATION OF YOUNG'S MODULUS, BOISE SANDSTONE.

again maximum values are to be found for the 4,000-psi confining pressure. Also shown in Table 3 are values of G calculated from Eq. 3 using values of E and υ calculated from Eqs. 1 and 2.

Poisson's ratios for the three sandstones were determined from plots of triaxial lateral strain vs triaxial longitudinal strain data shown in Figs. 20 through 22. These plots were generally curved and thus Poisson's ratio varies with strain (or with deviator stress). However, the curvature becomes less at higher values of strain. For purposes of comparison, an average straight line was drawn through the upper half of each curve, the slope determined and the average values of Poisson's ratios are reported in Table 3. Also reported are values of υ calculated from Eq. 2. These latter values again are averages for the upper half of the data.

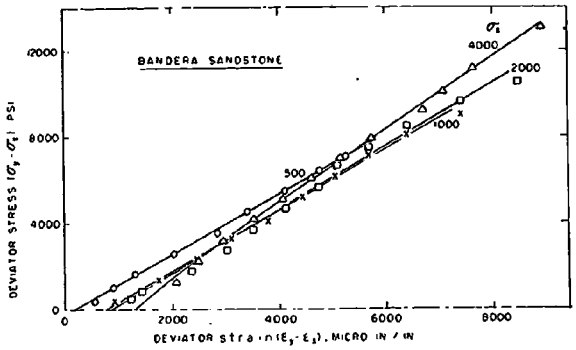

FIG. 17 — SHEAR MODULUS DETERMINATION, BANDERA SANDSTONE.

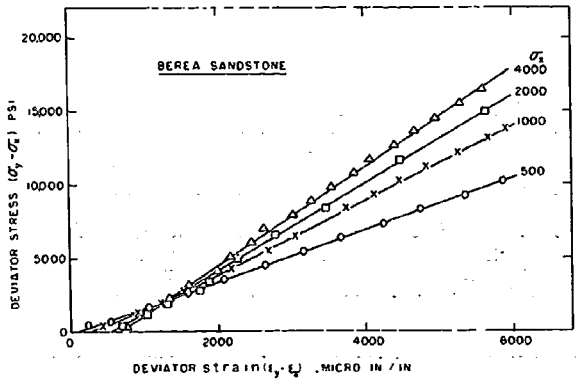

FIG. 18 — SHEAR MODULUS DETERMINATION, BEREA SANDSTONE.

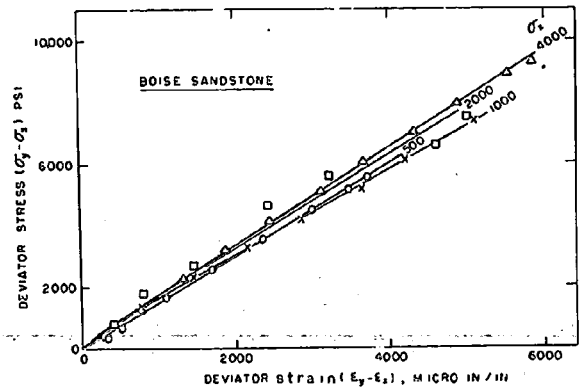

FIG. 19 — SHEAR MODULUS DETERMINATION, BOISE SANDSTONE.

DISCUSSION OF RESULTS

PORE PROPERTIES

The methods of measuring porosity and permea-

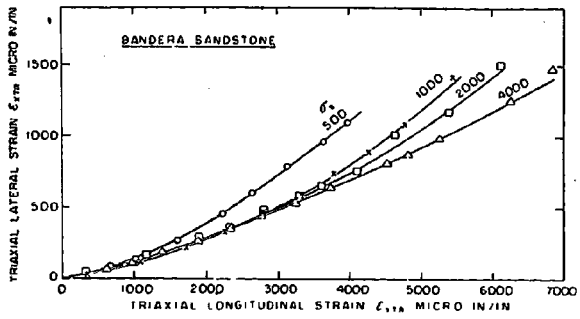

FIG. 20 — POISSON'S RATIO DETERMINATION, BANDERA SANDSTONE.

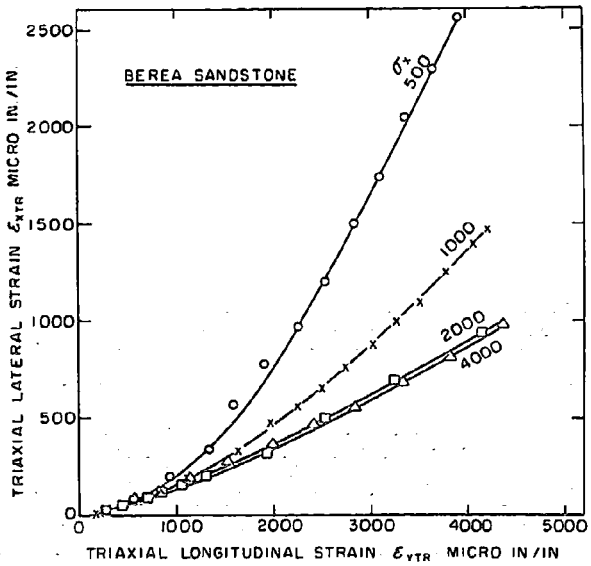

FIG. 21 — POISSON'S RATIO DETERMINATION, BEREA SANDSTONE.

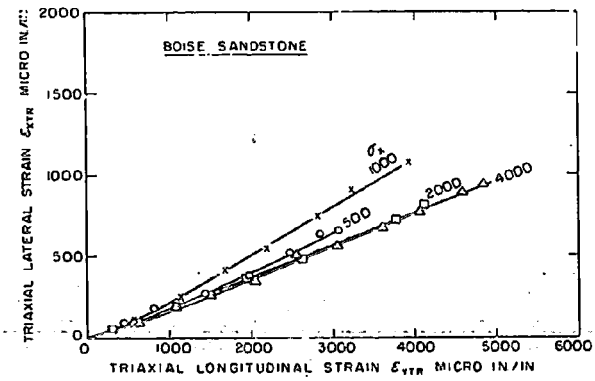

FIG. 22 — POISSON'S RATIO DETERMINATION, BOISE SANDSTONE.

bility under triaxial stress give results of good reproducibility (Figs. 12 and 13). Although smooth curves were drawn through the data points, it is possible that the systematic variations shown by the 4,000-psi confining pressure data have physical significance. Further tests would be necessary to confirm this point and to relate it to structural characteristics.

The greatest amounts of change in both porosity and permeability occur in the hydrostatic loading portion of the cycle. This was to be expected since it is generally found that the decrease of both porosity and permeability with increased stress is exponential. Thus, the large initial decrease should occur during hydrostatic loading. The relative positions of the curves are as expected, the greatest change occurring at the highest confining pressure. The absolute location of the curves, however, is determined partly by the nature of the test specimens and partly by the past stress history of the specimens. The only control that seemed practical in selecting test specimens was to use only those which had initial porosities and permeabilities within the smallest possible range. Great care was exercised in subjecting the samples to the same stress history as explained earlier.

Comparing present results with those of earlier investigators is complicated by several factors. Comparing hydrostatic test data with triaxial data is hardly possible unless the triaxial data are expressed as functions of some mean effective stress. By defining mean effective stress[11] as $\bar{\sigma} = (\sigma_y + 2\sigma_x)/3$, and replotting all data on this basis, good continuous curves result.

Comparing the hydrostatic portions of the present data with data analyzed by Dobrynin,[7] there is fairly good agreement except for the large reductions in permeability of Boise sandstone measured in the present work. These measured reductions were at least twice that noted for Dobrynin's most extreme case. The permeability reductions for Boise compared in magnitude with those observed by Bergamini[8] for low-permeability clay-bearing sandstones.

Comparing changes in porosity under triaxial loading with those measured by Handin[10] is complicated by the fact that his tests were run to much higher stress levels and the deformation was much more extreme. Thus, in general he observed larger changes in porosity during the deviatoric portion of the loading cycle than during the hydrostatic portion. However, his lack of prestressing the samples before making measurements may make comparisons invalid.

ELASTIC PROPERTIES

Measurements of elastic properties were subject to the same difficulties and restrictions as were porosity and permeability measurements. Strain stabilization was very important and so was the selection of comparable samples. Preloading of the sample for four cycles before making the measurements (Fig. 5) gave quite reproducible results. Samples were selected on the basis of their initial porosities and permeabilities, there being no way to preselect them on the basis of elastic characteristics. Of course, samples with obvious flaws were discarded.

The elastic data generally seem to be consistent although there is some scatter in the points, most notable at a confining pressure of 2,000 psi. No particular significance can be attached to this except to relate it to the characteristics of these particular samples. The curves are generally in the order which would be expected, but again their absolute locations are a function of the sample as well as of the confining pressure.

The Young's moduli and shear moduli both increase with increased confining pressure. This is as expected since increased confining pressure increases the strength of the sample. Agreement between triaxial moduli and values calculated as uniaxial equivalent values was fairly good except that the latter values were numerically smaller for Bandera and Berea and very nearly equal for Boise.

Poisson's ratio values are uncertain and show no consistent trend with confining pressure. Part of the difficulty lies in the fact that the strain data showed Poisson's ratio was not constant for a given confining pressure but varied with axial stress as well as with confining pressure. In general, the ratios of lateral strain to longitudinal strain increased with increased axial stress. Careful study of Cleary's[11] data also showed that the ratios are generally greater at higher values of mean effective stress. It was reported earlier[15] that Poisson's ratio increases with increased uniaxial stress.

Fig. 23 demonstrates clearly the strain anisotropy of Berea sandstone. For hydrostatic loading of an isotropic rock, lateral and longitudinal strains should be the same at equal values of stress. To test further the strain anisotropy of Berea sandstone, a hydrostatic loading test was run on a sample cut parallel to the bedding. There was still a difference between lateral and longitudinal strains,

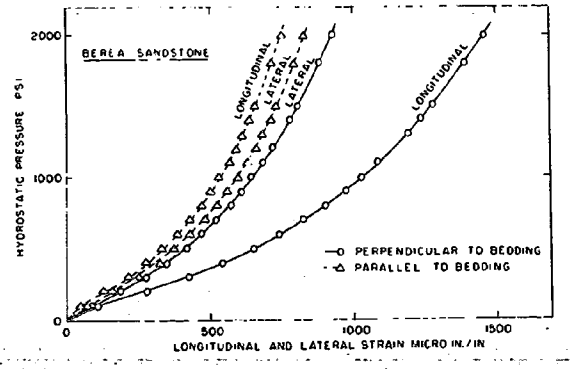

FIG. 23 — STRESS-STRAIN CURVES FROM HYDROSTATIC COMPRESSION OF BEREA SANDSTONE SAMPLES CUT PERPENDICULAR AND PARALLEL TO BEDDING.

but this difference was reduced in magnitude because of the averaging characteristics of the circumferential gauges used to measure lateral strains.

COMPARISON OF ELASTIC AND PORE PROPERTIES

Fig. 24 shows a comparison of changes in pore properties and elastic properties of the three sandstones as functions of confining pressure. Since no standard of comparison was available for elastic properties, absolute values of elastic moduli are plotted. The relations are generally as expected. Since the rigidity increases with increased confining pressure, there is less deformation of the sandstones and thus less change in porosity and permeability. Less change in pore properties would be expected for rocks having larger values of elastic moduli. This did not seem to be the case with the present samples. Initial values of porosity and permeability and other factors such as clay content and nature of the cementing materials, are probably of overriding importance.

It is unfortunate that Poisson's ratio data showed no consistent trend with confining pressure, for relations between Poisson's ratio and pore properties might be expected. For example, since changes in bulk volume of a rock reflect directly changes in pore volume, larger values of Poisson's ratio should be associated with smaller changes in porosity. This holds true for increasing axial stress at a given confining pressure. A relation between Poisson's ratio and permeability would be complex. On the other hand, if consideration were given to the greater distortion of pores which would result on the loading of material in which Poisson's ratio increases with stress, greater decrease in permeability would be expected. However, as with porosity, lesser decrease in pore size with increasing Poisson's ratio may also result in a lesser decrease in permeability with increased stress. Since these two effects work in opposite directions, they may tend to cancel each other and no meaningful relation between Poisson's ratio and permeability may exist.

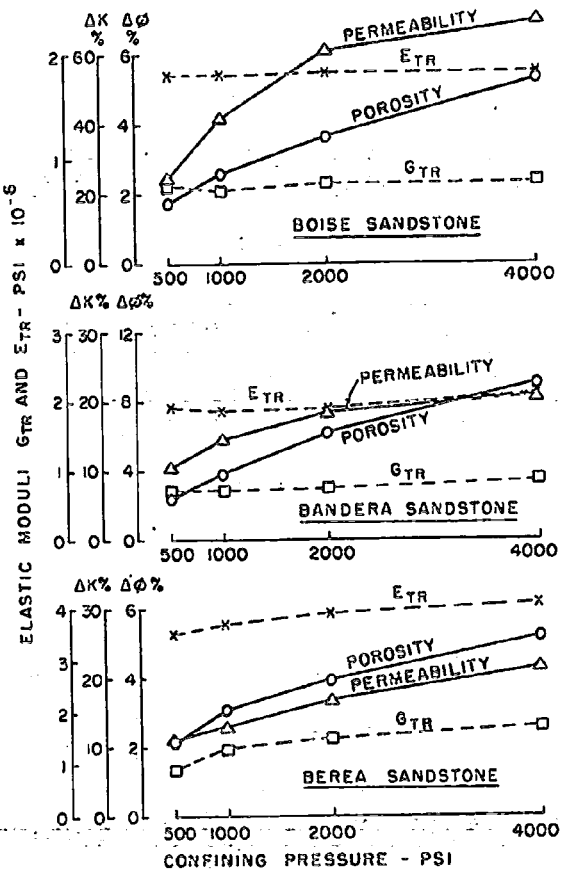

FIG. 24 — COMPARISON OF ELASTIC AND PORE PROPERTIES.

SUMMARY AND CONCLUSIONS

Equipment and methods have been developed for measurement of pore and elastic properties of rocks simultaneously under a wide range of triaxial loading conditions. The method is rapid considering the large amount of data which may be obtained in one run, and the results are quite reproducible.

Porosities and permeabilities of the three outcrop sandstones tested generally showed greater reduction during the hydrostatic portion than during the deviatoric portion of the triaxial loading cycle. However, upon application of deviator stress to approximately 80 percent of the ultimate triaxial strengths, substantial additional reductions in porosities and permeabilities occurred.

Triaxial elastic moduli (E_{TR} and G_{TR}) were calculated from measured strain gauge data. Triaxial Young's modulus (E_{TR}) is constant at a confining pressure of 4,000 psi. At lower confining pressures E_{TR} is somewhat dependent on axial stress but reaches a constant value at higher axial stress. The constant E_{TR} values increase in magnitude with confining pressure. Triaxial shear moduli are constant for a given confining pressure (independent of axial stress) but values of G_{TR} increase in magnitude with confining pressure. Poisson's ratios generally increase with increased axial stress but variation with confining pressure is not consistent.

There are very general relations between pore and elastic properties under triaxial stress conditions. The lesser decrease in porosity and permeability at higher stress values is related to the increase in rigidity of the rocks at higher stresses. The inconsistency of Poisson's ratio values made correlation with changes in pore properties almost impossible. Further work on these matters is indicated.

A number of other properties could be measured simultaneously with pore and elastic properties. The easiest of these to adapt to the present system would be dilatational and shear wave velocities by the method developed by King.[16]

ACKNOWLEDGMENTS

The North Atlantic Treaty Organization sponsored the principal author as a Research Fellow during the period of this research. A portion of the expense of the equipment and the technical assistance was provided by a grant from the National Science Foundation. The authors express their appreciation to both of these agencies.

REFERENCES

1. Jaeger, J. C.: "Brittle Fracture of Rocks", reprint of Eighth Symposium on Rock Mechanics, U. of Minnesota (Sept. 15-17, 1966).
2. Fatt, I. and Davis, D. H.: "Reduction in Permeability with Overburden Pressure", *Trans.*, AIME (1952) Vol. 195, 329.
3. McLatchie, A. S., Hemstock, R. A. and Young, J. W.: "The Effective Compressibility of Reservoir Rock and Its Effects on Permeability", *Trans.*, AIME (1958) Vol. 213, 386-388.
4. Knutson, C. F. and Bohor, B. F.: "Reservoir Rock Behavior Under Moderate Confining Pressure", *Fifth Symposium on Rock Mechanics*, Pergamon Press Ltd., New York (1963).
5. Wyble, D. O.: "Effect of Applied Pressure on the Conductivity, Porosity and Permeability of Sandstones", *Trans.*, AIME (1958) Vol. 213, 430-432.
6. Redmond, John C.: "Effect of Simulated Overburden Pressure on the Resistivity, Porosity and Permeability of Selected Sandstones", PhD Dissertation, Pennsylvania State U. (June, 1962).
7. Dobrynin, V. M.: "Effect of Overburden Pressure on Some Properties of Sandstone", *Soc. Pet. Eng. J.* (Dec., 1962) 360-366.
8. Bergamini, G.: "The Effect of Nonuniform Stress on Permeability of Sandstones", unpublished report, U. of California Petroleum Engineering Laboratories (May, 1962).
9. Gray, D. H., Fatt, I. and Bergamini, G.: "The Effect of Stress on Permeability of Sandstone Cores", *Soc. Pet. Eng. J.* (June, 1963) 95-100.
10. Handin, J. *et al.*: "Experimental Deformation of Sedimentary Rocks Under Confining Pressure: Pore Pressure Tests", *Bull.*, AAPG (May, 1963) Vol. 47, No. 5, 717.
11. Cleary, J. M.: "Hydraulic Fracture Theory: Part III. Elastic Properties of Sandstones", *Ill. State Geol. Surv. Circ. 281* (1959).
12. Wilhelmi, B.: "Simultaneous Measurement of Pore and Elastic Properties of Rocks Under Simulated Reservoir Stresses", MS Thesis, U. of California, Berkeley (June, 1966).
13. U. S. Corps of Engineers: "Strength Parameters of Selected Intermediate Quality Rocks", Engineer Study 552, Rock Mechanics Investigations, First Interim Report, MRD Laboratory 64/483 (July, 1966).
14. Yamasaki, T.: "Changes in Porosity and Permeability of Rocks Subjected to Deformation by Triaxial Loading", unpublished report, U. of California Petroleum Engineering Laboratories (Feb., 1965).
15. Somerton, W. H., Timur, A. and Gray, D. H.: "Stress Behavior of Rock under Drilling Loading Conditions", Paper SPE 166 presented at SPE Annual Fall Meeting, Dallas (Oct. 8-11, 1961).
16. King, M. S.: "Wave Velocities and Dynamic Elastic Moduli of Sedimentary Rocks", PhD Dissertation, U. of California, Berkeley (1964).

***